Ionized Gas Towards Molecular Clumps: Physical Properties of Massive Star Forming Regions

Katharine Johnston, Debra Shepherd, James Aguirre, Miranda Dunham, Eric Rosolowsky and Kenneth Wood

(St Andrews University and MPIA; NRAO; University of Pennsylvania; University of Texas at Austin and University of British Columbia at Okanagan)

University of St Andrews

ABSTRACT: This work aims to provide preliminary studies of a selection of sites containing intermediate- and high-mass star formation, specifically to uncover the presence of ionized gas towards them. We also wish to study the relationship between the star forming gas, traced by millimeter continuum emission from dust, and the ionized gas created by massive stars.

To fulfill these aims, we have conducted a search for ionized gas at 3.6 cm, using the Very Large Array, towards 31 intermediate- and high-mass clumps detected in previous millimeter continuum observations. Ten sources were selected from preliminary images from the Bolocam Galactic Plane Survey (BGPS, Aguirre et al. 2010, submitted), and 5 were selected from Beltran et al. (2006). The remaining 16 sources were observed serendipitously, as their positions lay within the observed VLA 3.6 cm fields.

We will select the most promising objects from this study for follow up with higher resolution observations, to map any outflows or disks towards these sources, and to study how the formation of an HII region affects the material within several hundreds of AU of the star. **Therefore, we selected sources that are within a declination range suitable for future study with Atacama Large Millimeter Array (ALMA) and the Expanded Very Large Array (EVLA).**

Note that, in this work, we adopt the terminology that a molecular core produces a single star (or close binary system) while molecular clumps form clusters of stars. In our study of massive star forming regions, our selected sources are several kiloparsecs away and, thus, we most likely detect clumps forming one or more massive stars along with many lower mass stars.

Table 1: Observed Millimeter Sources

Source Name (1)	R.A. (2000) (h m s) (2)	Decl. (2000) (° ′ ″) (3)	Gal. ℓ (deg) (4)	Gal. b (deg) (5)	v_{13CO} (km s^{-1}) (6)	d_{near} (kpc) (7)	d_{far} (kpc) (8)	Assumed Distance (9)	L_{IRAS} ($10^3 L_\odot$) (10)	$S_{1.1/1.2mm}$ (Jy) (11)	M ($M_\odot$) (12)	Ref. (13)	Source Type (14)
G044.521+00.387	19 11 24.7	+10 28 43	44.5211	0.3871	51.3 ± 0.7	$3.8^{+0.8}_{-0.6}$	8.3 ± 1.2	Near, H I SA	0.932–2.13	0.49 ± 0.11	56	BGPS	Serend.
G044.587+00.371	19 11 35.6	+10 31 47	44.5871	0.3711	16.3 ± 1.5	$1.2^{+0.3}_{-0.2}$	10.9 ± 1.4	Far, H I SA	...	0.56 ± 0.14	528	BGPS	Select.
G044.617+00.365	19 11 40.3	+10 33 13	44.6171	0.3652	17.7 ± 1.4	$1.3^{+0.3}_{-0.2}$	10.8 ± 1.4	Far, H I SA	...	0.16 ± 0.08	148	BGPS	Serend.
G044.661+00.351	19 11 48.3	+10 35 10	44.6611	0.3512	17.6 ± 1.8	$1.3^{+0.3}_{-0.2}$	10.8 ± 1.4	Far, H I SA	24.3–24.6	0.62 ± 0.12	574	BGPS	Select.
G048.540+00.040	19 20 19.9	+13 52 25	48.5405	0.0398	15.6 ± 1.5	$1.2^{+0.3}_{-0.2}$	10.0 ± 1.3	Far, H I SA	...	0.42 ± 0.12	333	BGPS	Serend.
G048.580+00.056	19 20 21.0	+13 54 59	48.5805	0.0558	16.2 ± 1.8	$1.2^{+0.3}_{-0.2}$	10.0 ± 1.3	Far, CA	...	3.16 ± 0.29	2508	BGPS	Select.
G048.598+00.252	19 19 40.3	+14 01 27	48.5984	0.2518	8.4 ± 2.4	0.6 ±0.2	10.6 ± 1.4	Far, CA	...	1.32 ± 0.23	1177	BGPS	Select.
G048.605+00.024	19 20 30.8	+13 55 21	48.6045	0.0238	18.0 ± 1.8	$1.4^{+0.3}_{-0.2}$	9.9 ± 1.3	Far, CA	927–932	7.36 ± 0.55	5725	BGPS	Serend.
G048.610+00.220	19 19 48.7	+14 01 11	48.6104	0.2198	9.2 ± 2.8	$0.7^{+0.3}_{-0.2}$	10.5 ± 1.4	Far, CA	...	0.24 ± 0.10	210	BGPS	Serend.
G048.616+00.088	19 20 18.2	+13 57 48	48.6165	0.0878	16.9 ± 1.3	$1.3^{+0.3}_{-0.2}$	10.0 ± 1.3	Far, CA	...	0.61 ± 0.13	484	BGPS	Select.
G048.634+00.230	19 19 49.3	+14 02 44	48.6344	0.2298	9.4 ± 3.6	0.7 ±0.3	10.5 ± 1.4	Far, CA	60.5–168	0.62 ± 0.14	543	BGPS	Serend.
G048.656+00.228	19 19 52.3	+14 03 51	48.6564	0.2278	12.7 ± 2.5	$1.0^{+0.3}_{-0.2}$	$10.3^{+1.4}_{-1.3}$	Far, CA	...	0.67 ± 0.16	564	BGPS	Select.
G048.751−00.142	19 21 24.0	+13 58 25	48.7506	−0.1421	66.3 ± 1.0	5.3 ± 0.7[a]	5.3 ± 0.7[a]	Far, H I SA	...	0.39 ± 0.12	87	BGPS	Select.
G048.771−00.148	19 21 27.6	+13 59 18	48.7706	−0.1481	66.9 ± 1.2	5.3 ± 0.7[a]	5.3 ± 0.7[a]	Far, H I SA	...	0.14 ± 0.08	31	BGPS	Serend.
G049.830+00.370	19 21 37.9	+15 10 03	49.8303	0.3703	5.2 ± 1.8	$0.4^{+0.2}_{-0.1}$	10.6 ± 1.4	Far, CA	127	1.09 ± 0.18	972	BGPS	Serend.
G049.912+00.370	19 21 47.5	+15 14 23	49.9123	0.3704	8.1 ± 1.4	$0.6^{+0.2}_{-0.1}$	$10.3^{+1.4}_{-1.3}$	Far, H I SA	7.61–21.2	0.50 ± 0.13	421	BGPS	Select.
G050.271−00.442	19 25 27.5	+15 10 18	50.2706	−0.4415	14.8 ± 1.3	1.2 ± 0.2	9.7 ± 1.3	Far, H I SA	0.960–254	0.21 ± 0.10	157	BGPS	Select.
G050.283−00.390	19 25 17.6	+15 12 25	50.2826	−0.3895	16.1 ± 1.5	$1.3^{+0.3}_{-0.2}$	9.6 ± 1.3	Far, CA	281–286	1.40 ± 0.21	1024	BGPS	Select.
IRAS 18256−0742 Clump 1	18 28 18.9	−07 40 06	23.4730	1.6041	...	3.0	...	Near, B06	10.5	0.59	52	B06	Select.
IRAS 18424−0329 Clump 2	18 45 00.5	−03 27 04	29.1280	−0.1449	47.4 ± 1.5	3.2 ± 0.5	11.6 ± 1.5	Far, H I SA	55[b]	0.53	710	B06	Select.
IRAS 18424−0329 Clump 4	18 45 01.6	−03 27 20	29.1261	−0.1510	47.6 ± 1.4	3.2 ± 0.5	11.6 ± 1.5	Far, H I SA	55[b]	0.28	372	B06	Serend.
IRAS 18424−0329 Clump 6	18 45 00.5	−03 27 36	29.1201	−0.1490	47.6 ± 1.7	3.2 ± 0.5	11.6 ± 1.5	Far, H I SA	55[b]	0.24	326	B06	Serend.
IRAS 18571+0349 Clump 1	18 59 42.7	+03 53 42	37.3409	−0.0615	55.5 ± 1.0	$3.7^{+0.6}_{-0.5}$	9.8 ± 1.3	Far, KB94	106	1.55	1509	B06	Select.
IRAS 18571+0349 Clump 3	18 59 49.0	+03 56 30	37.3944	−0.0635	56.7 ± 2.6	$3.8^{+0.7}_{-0.6}$	9.7 ± 1.3	Far, KB94	...	0.31	291	B06	Select.
IRAS 18571+0349 Clump 4	18 59 51.2	+03 55 18	37.3808	−0.0808	57.1 ± 1.1	$3.8^{+0.7}_{-0.6}$	9.7 ± 1.3	Far, KB94	...	0.23	217	B06	Serend.
IRAS 18586+0106 Clump 1	19 01 15.8	+01 12 28	35.1276	−1.6345	...	2.7	...	Near, B06	...	1.47	110	B06	Select.
IRAS 18586+0106 Clump 3	19 00 59.8	+01 13 40	35.1150	−1.5661	...	2.7	...	Near, B06	...	0.43	32	B06	Serend.
IRAS 18586+0106 Clump 4	19 01 01.4	+01 13 16	35.1121	−1.5751	...	2.7	...	Near, B06	...	0.52	39	B06	Serend.
IRAS 18586+0106 Clump 5	19 01 12.1	+01 10 44	35.0949	−1.6340	...	2.7	...	Near, B06	4.4	0.49	36	B06	Serend.
IRAS 18586+0106 Clump 6	19 01 27.0	+01 10 28	35.1193	−1.6912	...	2.7	...	Near, B06	...	0.30	22	B06	Serend.
IRAS 18586+0106 Clump 7	19 00 59.3	+01 11 08	35.0765	−1.5835	...	2.7	...	Near, B06	...	0.21	16	B06	Serend.

Notes. Columns: 1. Millimeter clump name. 2. and 3. Equatorial J2000 coordinates of millimeter clump. 4. and 5. Galactic coordinates of millimeter clump. 6. Mean velocity of associated GRS ^{13}CO emission at position of mm source. 7. and 8. Near and far distance to millimeter clump in kpc. 9. Assumed distance used to calculate the *IRAS* luminosity and clump mass. The method used to determine whether the source is at the near or far distance is also given. H I SA: H I self-absorption, CA: 21 cm continuum absorption, B06: taken from B06, KB94: Kuchar & Bania (1994). 10. Luminosity derived from associated *IRAS* source fluxes. 11. Millimeter flux measured at a wavelength of 1.1 mm for the sources taken from the BGPS, and 1.2 mm for those taken from B06. 12. The calculated dust mass of the millimeter clump. 13. References – BGPS: Bolocam Galactic Plane Survey preliminary images, J. E. Aguirre et al. (2010, submitted). B06: Beltrán et al. (2006) 14. Denotes whether source was selected (Select.) or serendipitously fell within the VLA field (Serend.).

[a] The velocity of this source is too high to be explained by the galactic rotation curve at this galactic longitude, therefore the highest possible velocity at this longitude was instead assumed. These sources were originally thought to be at a different velocity, placing them at $d_{near} \sim 1$ kpc.

[b] It is not certain which of the clumps listed by B06 is associated with IRAS 18424−0329, however the general 1.2 mm emission in this field is coincident with the *IRAS* source.

The selected molecular clumps have masses large enough to harbor forming intermediate or high-mass stars, ranging from approximately 16 to 5700 $M_\odot$

The BGPS

The BGPS (Aguirre et al. 2010, submitted) is a 1.1 mm continuum survey of 170 square degrees of the Galactic Plane visible from the northern hemisphere, including a contiguous strip from l = -10.5 to 90.5, b = ±0.5, as well as selected regions beyond the solar circle. The survey has a limiting non-uniform 1-σ noise level in the range 11 and 53 mJy/beam RMS at an effective resolution of 33".

Observations from Beltran et al. (2006)

The observations of B06 were taken with the 37-channel SEST Imaging Bolometer Array (SIMBA) on the Swedish-ESO Submillimetre Telescope (SEST) to identify 1.2 mm continuum emission within a 15' by 6.6' region centered on selected IRAS sources. These observations have a resolution of 40".

A survey specifically designed for follow up with the eVLA and ALMA

The survey was specifically designed so that selected sources could be followed up with both the eVLA and ALMA i.e. they were selected within the declination ranges of both telescopes.

Follow up observations with eVLA

Radio continuum observed with the eVLA will be x10 more sensitive than the current VLA.

- will detect even fainter extended emission from the ionized gas associated with young massive stars
- a 1 hr integration at 3.6 cm in D array will be able to detect an unresolved UC HII region created by a B2 ZAMS star at 12 kpc!

Follow up observations with ALMA

Observations of an outflow and core, example setup:

- **Band 6** (211-275 GHz) ⇒ 27" primary beam
- **5'x5' mosaic** ⇒ 625 fields, if Nyquist sampled at 12"
- **Spatial resolution**: 1.3 - 0.014", depending on array configuration, with LAS=18" **BUT** combine with ACA
  - ⇒ **Recover all size scales! Recover all flux!**
  - ⇒ **More accurate mass/outflow dynamics estimates**
- **Correlator setup:** observe lines in 2 sidebands, such as: ^{12}CO(2-1), ^{13}CO, $C^{18}O$, $C^{17}O$, HCN(3-2), HCO^+(3-2), CH_3CN, CH_3OH... and 2x 2GHz BW continuum bands
- **Sensitivity:** 8 hrs total (46m per field)
  - ⇒ RMS= 15 mJy/bm in lines with e.g. 0.5 MHz or 0.68 km/s res.
  - ⇒ RMS= 0.17 mJy/bm in continuum (both for ALMA array only)

Observations of a disk, outflow, and inner core, example setup:

- **Band 7** (275-373 GHz) ⇒ 18" primary beam
- **Single field**
- **Spatial resolution:** 1.0 - 0.011" (e.g. as good as 30AU at 2kpc!)
  - ⇒ **Can study disk kinematics and outflow launching region**
- **Correlator setup**: observe lines in 2 sidebands, such as: ^{12}CO(3-2), ^{13}CO, HCOOCH$_3$, H^{13}CN, CS(7-6), CH$_3$CN(18-17)... and 2x 2GHz BW continuum bands
- **Sensitivity:** 1 hr integration time
  - ⇒ RMS= 3.4 mJy in lines with e.g. 0.5 MHz or 0.58 km/s res.
  - ⇒ RMS= 0.038 mJy for continuum (both for ALMA array only)

An example of one of the observed fields

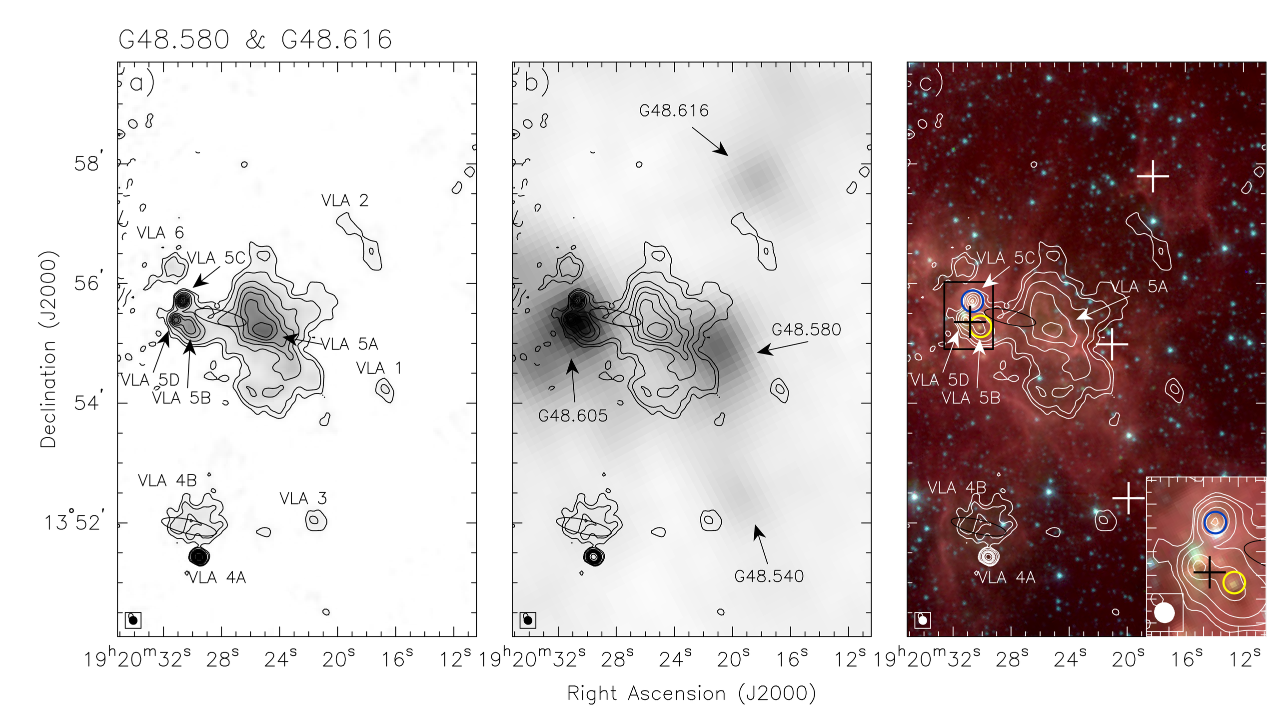

Figure 2.2: a) 3.6 cm continuum, b) 1.1 mm, and c) GLIMPSE images of the G48.580 & G48.616 field. Each image is overlaid with contours of 3.6 cm continuum emission. The detected 3.6 cm and 1.1 mm sources are labeled in panels a) and b) respectively. Panel a) Contour levels: -3, 3, 5, 10, 15, 20, 25, 30, 35, 40, 60 $\times \Delta S = 1.2$ mJy beam^{-1}. Synthesised beam: 9.1 × 8.7" P.A.=56 degrees. Range of greyscale: 1.2 - 68 mJy beam^{-1}. Panel b) Contour levels and beam as in a). Range of greyscale: -0.06 - 1.3 Jy beam^{-1}. Panel c) Contour levels: 3, 5, 10, 20, 30, 40, 60 $\times \Delta S = 1.2$ mJy beam^{-1}. Synthesised beam: 9.1 × 8.7" P.A.=56 degrees. GLIMPSE image stretch: logarithmic, R: 20-1300, G: 2-600, B: 2-1000 MJy Sr^{-1}.

In the 10 observed fields, 35 HII regions are identified, of which 20 are newly discovered.

Here we present one of the observed fields, comparing its cm, mm and mid-IR emission.

Throughout the observed fields, there is a large range in the properties of the detected HII regions; their physical sizes extend from <0.05 pc to 7.88 pc, and their spectral types cover B2 to O5.

Figure 2.2: The G48.580 & G48.616 field
Left panel: Contours and Grayscale: VLA 3.6 cm D-array continuum emission of the G48.580 & G48.616 field. VLA 3.6 cm sources are labeled.
Middle panel: Contours: as on left panel, Grayscale: Bolocam Galactic Plane Survey 1.1 mm image. Millimeter sources are labeled.
Right panel: Mid-IR GLIMPSE image of the G48.580 & G48.616 field. Main panel: three-colour GLIMPSE image (Red:8μm, Green:4.5μm, Blue: 3.6μm). Contours: VLA 3.6 cm D-array continuum emission. Inset: Close-up of sources VLA 5B, 5C, and 5D covering the area shown by the black box in the main panel. Crosses mark the peak positions of Bolocam millimeter sources (in increasing R.A.: G48.616, G48.540, G48.580, G48.605).
All panels: Ellipses mark the positions of any associated IRAS sources.

Discussion of images:
If the centimeter emission from each of the subcomponents of VLA 5 is created by a single star, these HII regions have been created by a cluster of late O-type stars.

The edge of VLA 5A is associated with the millimeter source G48.580, but the morphology of the 3.6 cm emission suggests that the clump G48.580 may instead be inhibiting the expansion of the HII region traced by VLA 5A. The sources VLA 5B, VLA 5C, and VLA 5D are associated with the millimeter clump G48.605.

Comparison between the GLIMPSE and VLA 3.6 cm images reveals that VLA 5B is associated with the GLIMPSE source SSTGLMC G048.6021+00.0257, and VLA 5C is associated with the GLIMPSE source SSTGLMC G048.6093+00.0270 (whose positions are shown by a yellow and blue circle respectively in the top right panel). There are no mid-IR IRAC sources directly associated with the peak of the compact HII region VLA 5D, in fact the source appears to lie within a dark filament.

However, VLA 5D appears to have associated 4.5 μm emission (green) extending in the NW-SE direction. Emission in the 4.5 μm band is thought to be produced by shocked H_2 or CO gas in outflows (see Cyganowski et al. 2008, and references within). Both water and OH masers have been detected towards VLA 5D (e.g. Forster & Caswell 1989). If we are seeing shocked gas from the outflow of this source, this provides further evidence towards its youth, and suggests it may still be in the process of outflow and accretion.

Relationships between the properties of the molecular and ionized gas

Of the 31 millimeter clumps observed, 9 of these appear to be physically related to ionized gas, and a further 6 have ionized gas emission within 1'.

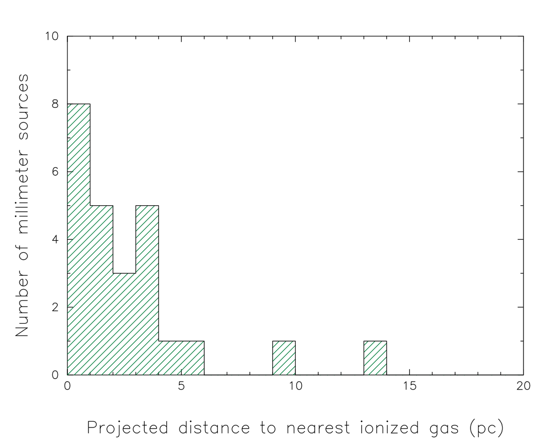

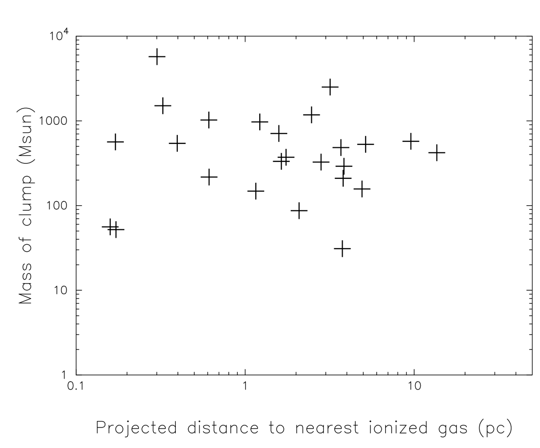

Top Left Figure: The distribution of mm clumps as a function of the projected distance to the peak of their nearest 3.6 cm emission in parsecs.

Top Right Figure: Mass of selected millimeter sources as a function of the projected distance to their nearest ionized gas in parsecs.

Conclusion: The ionized gas is preferentially associated toward millimeter clumps, however this does not depend on the mass of the clump.

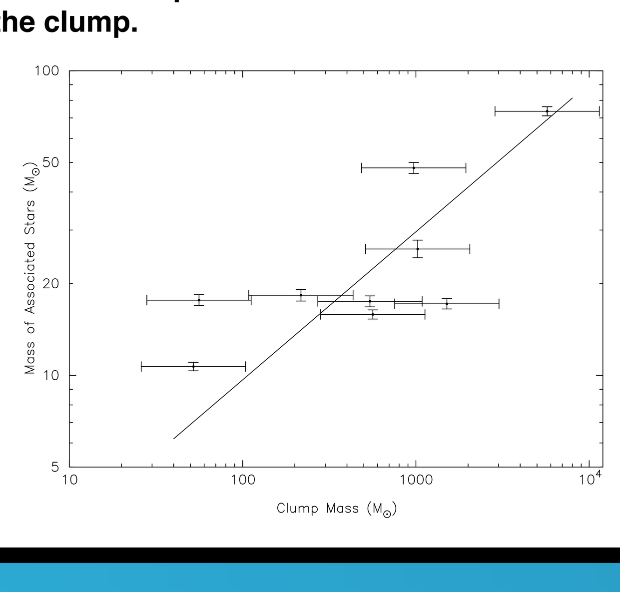

Bottom Left Figure: The relationship between the mass of clumps associated with ionized gas, M_{clump}, and the mass of their embedded stars, $M_\star$. The combined stellar mass $M_\star$ was derived from the luminosities of the exciting stars, which were calculated from the cm continuum emission.

This Figure shows a possible power law relationship between M_{clump} and $M_\star$. These data can be fit by the following power law: $M_\star = 1.0 \pm 0.9 \times M_{clump}^{\,0.5 \pm 0.1}$, drawn upon the data.

This result is consistent with the idea that the mass of the clump determines the mass of the massive stars forming within it. A similar relationship was found by Ho et al. (1981), using a comparable number of observed HII regions. Larson (1982) also discovered a similar result when comparing the mass of the most massive star in nearby young clusters to their associated cloud masses, finding $M(max) = 0.33 \times M_{cloud}^{0.43}$. In addition, Larson (2003) found a relationship between the most massive star and the total stellar mass of these clusters, given by $M(max) \propto 1.2 \times M_{cluster}^{\,0.45}$. This M(max)-$M_{cluster}$ relation has also been studied more recently by Weidner et al. (2010), who find that it cannot be explained by random sampling of an IMF, and may in fact be a relationship which probes the physical conditions **required** to form massive stars, i.e. more massive cluster-forming clouds.

Summary and conclusions

- We have conducted 3.6cm VLA observations towards 31 millimeter clumps detected previously in millimeter continuum (Aguirre et al. 2010, submitted, and Beltran et al. 2006).
- In the 10 observed fields, 35 HII regions are identified, of which 20 are newly discovered. Many of the HII regions are multiply peaked indicating the presence of a cluster of massive stars.
- We describe and compare the 3.6cm and 1mm images for one of the observed fields. We also compare the ionized gas emission to GLIMPSE images of this region.
- We have detailed some example observing setups for follow-up observations of several of these sources with ALMA, to observe any associated outflows and the dense accreting material within several 100 AU of the central protostar.
- Of the 31 millimeter clumps observed, 9 of these appear to be physically related to ionized gas, and a further 6 have ionized gas emission within 1'. Further, we find that the ionized gas is preferentially associated towards the millimeter clumps, yet this is not dependent on the mass of the clump.
- We find a correlation between the clump mass and the mass of the ionizing massive stars within it, which is described by a power law. This result is consistent with the idea that the mass of the clump determines the mass of the massive stars forming within it. In future, we plan to investigate this relation with a larger number of clumps.

This work is published in ApJ: Johnston et al. 2009, ApJ 707, 283

Please email any questions or comments to: kgj1@st-andrews.ac.uk